Biochimica et Biophysica Acta 1843 (2014) 2730–2743

Contents lists available at ScienceDirect

Biochimica et Biophysica Acta

journal homepage: www.elsevier.com/locate/bbamcr

Hypoximimetic activity of *N*-acyl-dopamines. *N*-arachidonoyl-dopamine stabilizes HIF-1α protein through a SIAH2-dependent pathway

Rafael Soler-Torronteras, Maribel Lara-Chica, Victor García, Marco A. Calzado *, Eduardo Muñoz *

Instituto Maimónides de Investigación Biomédica de Córdoba (IMIBIC)/ Hospital Universitario Reina Sofía/ Universidad de Córdoba, Córdoba, Spain

ARTICLE INFO

Article history:
Received 21 March 2014
Received in revised form 11 July 2014
Accepted 15 July 2014
Available online 2 August 2014

Keywords:
Endogenous lipid mediator
Signal transduction
Hypoxia
Neuroprotection

ABSTRACT

The *N*-acyl conjugates of amino acids and neurotransmitters (NAANs) are a class of endogenous lipid messengers that are expressed in the mammalian central and peripheral nervous system. Hypoxia inducible factor-1α (HIF-1α) is a transcription factor that plays a key role in the cellular adaptation to hypoxia and ischemia, and hypoxic preconditioning through HIF-1α has been shown to be neuroprotective in ischemic models. This study showed that *N*-acyl-dopamines induce HIF-1α stabilization on human primary astrocytes and neurons as well as in transformed cell lines. *N*-arachidonoyl-dopamine (NADA)-induced HIF-1α stabilization depends on the dopamine moiety of the molecule and is independent of cannabinoid receptor-1 (CB_1) and transient receptor potential vanilloid type I (TRPV1) activation. NADA increases the activity of the E3 ubiquitin ligase seven in absentia homolog-2 (SIAH2), inhibits prolyl-hydroxylase-3 (PHD3) and stabilizes HIF-1α. NADA enhances angiogenesis in endothelial vascular cells and promotes the expression of genes such as erythropoietin (EPO), vascular endothelial growth factor A (VEGFA), heme oxygenase 1 (HMOX-1), hexokinase 2 (HK2) and Bcl-2/E1B-nineteen kiloDalton interacting protein (BNIP3) in primary astrocytes. These findings indicate a link between *N*-acyl-dopamines and hypoxic preconditioning and suggest that modulation of the *N*-acyl-dopamine metabolism might prove useful for prevention against hypoxic diseases.

1. Introduction

The *N*-acyl conjugates of amino acids and neurotransmitters (NAANs) include compounds such as glycine, GABA or dopamine conjugated with long chain fatty acids. A large number of endogenous NAANs have been reported although their physiological role remains largely unknown [1]. Among them *N*-arachidonoyl-dopamine (NADA) and *N*-oleyl-dopamine (OLDA) have attracted special interest because they have been identified in brain homogenates and target receptors of the endocannabinoid system [2]. While NADA binds to cannabinoid type 1 receptor (CB_1) and the transient receptor potential vanilloid type 1 channel (TRPV-1) [2–4], OLDA is a capsaicin-like lipid with full TRPV-1 agonist activity but devoid of affinity for CB receptors [5].

NADA has been identified in the striatum, hippocampus, cerebellum and the dorsal root ganglion and is proposed to play a role in neuronal pain and inflammation [2]. In different experimental models it has been shown that NADA is a pleiotropic endocannabinoid/endovanilloid that exerts biological activities through mechanisms that are dependent and independent of CB_1 and TRPV-1 receptors. NADA had anandamide (AEA)-like activity in mice, producing the classic tetrad of behavioral signs characteristic of cannabinoid agonists such as increased immobility in the ring test, decreased body temperature, reduced locomotor activity and delayed response to a thermal stimulus [4]. In addition NADA induces hyperalgesia [2], smooth muscle contraction in the guinea pig bronchi and bladder [6], vasorelaxation in blood vessels [7], oxidative stress and apoptosis in hepatic stellate cells [8] and also has anti-HIV-1, neuroprotective and antiinflammatory properties [9–13]. Their saturated analogs *N*-palmitoyl-dopamine (PALDA) and *N*-stearoyl-dopamine (STEARDA) were also identified as endogenous substances not activating TRPV-1, although they significantly enhanced the TRPV-1-mediated effects of NADA [5].

Endocannabinoids as well as other NAANs may play a major role in neuroprotection by regulating the cellular network of communication between the nervous and immune system during neuroinflammation and neuronal damage [14]. However, the exact mechanisms by which

Abbreviations: AEA, *N*-arachidonoyl-ethanolamide; BNIP3, Bcl-2/E1B-nineteen kiloDalton interacting protein; CB1, cannabinoid receptor-1; EPO, erythropoietin; HBMECs, human brain microvascular endothelial cells; HUVECs, human umbilical vein endothelial cells; HIF, hypoxia inducing factor; HK2, hexokinase 2; HMOX-1, heme oxygenase 1; NADA, *N*-arachidonoyl-dopamine; NAANs, *N*-acyl conjugates of amino acids and neurotransmitters; NF-κB, nuclear factor *kappa* B; PALDA, *N*-palmitoyl-dopamine; OLDA, *N*-oleyl-dopamine; PHD3, prolyl-hydroxylase-3; SIAH2, seven in absentia homolog-2; STEARDA, *N*-stearoyl-dopamine; TRPV1, transient receptor potential vanilloid; VEGFA, vascular endothelial growth factor A

* Corresponding authors at: Departamento de Biología Celular, Fisiología e Inmunología, Facultad de Medicina, Universidad de Córdoba, C/María Virgen y Madre s/n., 14004 Córdoba, Spain. Tel.: +34 957218267; fax: +34 957218266.

E-mail addresses: mcalzado@uco.es (M.A. Calzado), e.munoz@uco.es (E. Muñoz).

http://dx.doi.org/10.1016/j.bbamcr.2014.07.005
0167-4889/

different endocannabinoids and NAANs provide neuroprotection are far to be understood.

Hypoxia-inducible factor (HIF)-1 mediates the endogenous adaptive program to hypoxia, and manipulation of components of the HIF-1 pathway results in neuroprotection in different experimental models [15]. Therefore the development of novel compounds with hypoximimetic activity is of interest for the treatment of hypoxic CNS diseases. In the context of deprivation of oxygen, cells adapt through up-regulation of the HIF-1α protein, which, together with HIF-1β forms the transcription factor HIF-1 [16,17]. Under normoxic conditions, HIF-1α levels are controlled by hydroxylation on proline 402 and 564 mediated by prolyl-hydroxylases (PHDs), which function as oxygen sensors [18]. The hydroxylated HIF-1α increased its affinity for the tumor-suppressor protein von Hippel–Lindau (VHL), a component of an E3 ubiquitin ligase complex together with elongin B, C and cullin [19–21]. This complex mediates poly-ubiquitination of HIF-1α, which causes its degradation by the 26S proteasome [22]. On the other hand, under hypoxic conditions HIF-1α hydroxylation is decreased because reduced steady state levels of PHDs, which is controlled by SIAH (seven in absentia homolog) proteins by poly-ubiquitination and proteosomal degradation [23]. Low levels of oxygen cause the association between PHD3 and SIAH2, which favors the incorporation of other PHDs, resulting in the degradation of these enzymes and subsequent HIF-1α stabilization. In summary, SIAH2 plays a key role in the regulation of hypoxia response by modulating HIF-1α stability. This role was confirmed by the analysis of Siah2$^{-/-}$ mice, which show a blunted response to hypoxia [23]. Similarly, the interference of SIAH2/PHD binding reduces hypoxia-mediated up-regulation of HIF-1α and impairs neoangiogenesis in a syngeneic mouse model [24].

The SIAH protein family belongs to the RING (Really Interesting New Gene) finger E3 ubiquitin ligases, which in humans is formed by two subunits (SIAH1 and SIAH2) with similar and redundant functions encoded by different genes [25–28]. SIAH2 is responsible for ubiquitination and proteosomal degradation of specific substrates, interacting with them either directly or through adapter proteins [29–32]. SIAH2 substrates are involved in important signaling pathways that have been described, such as PHDs, PML, HDAC3, β-catenin, HIPK2 and DYRK2 [23,29,31,33–35]. SIAH2 expression and activity could be regulated at different levels. It has been described that SIAH2 levels are modulated at the transcriptional level by estrogens [17] and in response to transcription factors such as WNT5a and E2F1 [36,37]. In the same sense, the small noncoding microRNA MiR-146b targets the SIAH2 mRNA for degradation in response to TGFβ signaling [38]. At the protein level, different post-translational modifications have been described for SIAH2, its capacity to control their availability and activity by autoubiquitination being the most relevant under normal physiological conditions [39]. Under stress conditions, SIAH2 levels could be modulated by phosphorylation performed by upstream kinases. For instance, SIAH2 is phosphorylated by p38 MAPK, increasing its ability to degrade PHD3 [40]. Moreover, we have previously showed that two members of the dual-specificity tyrosine-regulated kinase (DYRK) family, HIPK2 and DYRK2, induce a strong phosphorylation of SIAH2 modifying its activity [29,35]. Several peptides able to modify SIAH2 activity have been described [24,41]. However, vitamin K3 (menadione) is to date the only chemical compound described able to affect SIAH2 levels and activity through a redox-independent mechanism [42].

The aims of this study were to determine the capacity of *N*-acyl-dopamines and related lipids to regulate hypoxia-dependent mechanisms in neuronal and non-neuronal cells. Herein we show for the first time that *N*-acyl-dopamines mediate HIF-1α stabilization through CB_1- and TRPV-1-independent mechanisms. Moreover, we demonstrate that NADA specifically increases the activity of SIAH2 enhancing PHD3 degradation. As a consequence, NADA acts as a hypoximimetic agent, regulating a large number of genes involved in the hypoxia response and inducing angiogenesis in primary vascular endothelial cells. Our results provide new insights into the neuroprotective mechanisms of *N*-acyl-dopamines and open new research avenues for the development of novel therapeutic strategies for the management of CNS diseases.

2. Material and methods

2.1. Cell cultures

HEK-293T, HeLa, SK-N-SH, U87, MO3.13, control MEFs (mouse embryonic fibroblasts) and Siah1a$^{-/-}$/Siah2$^{-/-}$ MEF cells were maintained in DMEM medium supplemented with 10% FBS and 1% (v/v) penicillin/streptomycin at 37 °C in a humidified atmosphere containing 5% CO_2. HUVECs were maintained in medium 199 supplemented with 20% FBS, 2 mM penicillin/streptomycin (10,000 U and 10 mg/ml, respectively), 2 mM amphotericin B, 2 mM L-glutamine, 10 mM Hepes, 30 mg/ml ECGS, and 100 mg/ml heparin. Primary cells were purchased from ScienCell (Carlsbad, CA, USA). Human brain microvascular endothelial cells (HBMECs) were maintained in endothelial cell medium (ScienCell, P60104) supplemented with 5% FBS, 1% ECGS and 1% penicillin/streptomycin. Human astrocytes were maintained in astrocyte medium (ScienCell, P60101) supplemented with 2% FBS, 1% AGS and 1% penicillin/streptomycin solution. Human neurons from cortex were maintained in neuronal medium (ScienCell, P60157) supplemented with 1% NGS and 1% P/S solution. Hypoxia was induced by the culture of cells in a New Brunswick Galaxy 48R incubator at 1% O_2 concentration.

2.2. Transfection, plasmids and reagents

Transient transfections were carried out with Roti-Fect (Carl Roth) and harvested between 36 and 48 h after transfection. DNA amounts in each transfection were kept constant after the addition of empty expression vector. Flag-SIAH2, HA-SIAH2, Flag-SIAH2 RM (Ring Mutant, H98A/C101A), Flag-SIAH-5A (Ser16, Thr26, Ser28, Ser68, and Thr119 to alanine), Flag SIAH-5D (Ser16, Thr26, Ser28, Ser68, and Thr119 to aspartic acid) and HA-Ubiquitin were previously described [29,35]. Flag-PHD3 was a gift from Dr. Frank S. Lee (Pennsylvania School of Medicine) and Epo-Luc was a gift from Dr. M. L. Schmitz (Univ. of Giessen, Germany). *N*-arachidonoyl-dopamine (NADA), *N*-oleoyl-dopamine (OLDA), dopamine and cycloheximide were from Sigma-Aldrich (St. Louis, MO, USA). *N*-palmitoyl-dopamine (PALDA) and AM251 were from Cayman Chemicals (Ann Arbor, MI, USA). *N*-stearoyl-dopamine (STEARDA) was from Tocris Bioscience (Bristol, UK). *N*-arachidonoyl-L-tyrosine, *N*-arachidonoyl-ethanolamide (AEA), *N*-(4-hydroxyphenyl)-arachidonoyl ethanolamide (AM404), LY 294002 and MG-132 were from Enzo Life Science (Lausen, Switzerland). SB705498 was from Selleck Chemicals LCC (Houston, TX, USA). Hydroxytyrosol esters were a gift from Prof. Giovanni Appendino (UNIPMN, Novara, Italy). Scramble control oligonucleotide siRNA non-targeting pool (D-001810-10-20) and the siGENOME SMARTpool against SIAH2 (M-006561-02) were purchased from Dharmacon (Waltham, MA, USA).

2.3. Western blotting and antibodies

Protein soluble fractions were obtained by lysing the cells in 100 μl of NP-40 buffer (50 mM Tris–HCl pH 7.5, 150 mM NaCl, 10% glycerol and 1% NP-40) supplemented with 10 mM NaF, 1 mM Na_3VO_4, 10 μg/ml leupeptine, 1 μg/ml pepstatin and aprotinin, and 1 μl/ml PMSF saturated. After centrifugation the supernatants were mixed with SDS sample buffer and boiled at 95 °C. Proteins were electrophoresed in 8–10% sodium dodecyl sulfate polyacrylamide gel (SDS-PAGE) and transferred to polyvinylidene difluoride membranes (20 V and 30 min per membrane). After blocking with non-fat milk or BSA in TBST buffer, primary antibodies were added. The washed membranes were incubated with appropriate secondary antibodies coupled to horseradish peroxidase

that were detected by an enhanced chemiluminescence system (USB). Antibodies against the FLAG epitope (clone M2) and anti-β-actin (AC-74) were purchased from Sigma-Aldrich. Anti-SIAH2 (sc-5507) and anti-DYRK2 (sc-66867) was obtained from Santa Cruz (Santa Cruz, CA, USA). Anti-HIPK2 was a gift from Dr. M. L. Schmitz and has been described previously [43]. Anti-HA epitope (clone 3F10) was purchased from Roche Molecular Biochemicals (Mannheim, Germany). Anti HIF-1α (610959) was from BD Biosciences (Madrid, Spain), anti-PHD3 (ab30782) and anti-PHD2 (ab109088) from Abcam (Cambrigde, UK), and anti-phospho-Akt Ser473 (9271) from Cell Signaling Technology (Danvers, MA, USA).

2.4. Immunoprecipitation

Cells were washed in PBS, collected by centrifugation and the pellet was lysed in IP buffer (50 mM Hepes pH 7.5, 50 mM NaCl and 1% Triton X-100) supplemented with 5 mM EGTA, 20 mM $Na_4P_2O_7$, 50 mM NaF, 1 mM Na_3VO_4, 2 mM PMSF and 10 μg/ml of leupeptine, aprotinin and pepstatin. Before immunoprecipitation, cell lysates were pre-cleared with protein A/G PLUS agarose (Santa Cruz). Lysates were incubated with 1 μg of antibody together with 25 μl of the protein A/G. After rotating for 4 h at 4 °C, the beads were washed 5 times in IP buffer and eluted in 1.5× SDS sample buffer, followed by western blotting.

2.5. Luciferase reporter assays

Cells were collected, washed in PBS and lysed in luciferase buffer (25 mM Tris–phosphate pH 7.8, 8 mM $MgCl_2$, 1 mM DTT, 1% Triton X-100, and 7% glycerol). Luciferase activity was measured using an Autolumat LB 953 (EG&G Berthold, USA) following the instructions of the luciferase assay kit (Promega, Madison, WI, USA).

2.6. RNA extraction and qRT-PCR

Cells were collected in PBS and total RNA was extracted using the High Pure RNA Isolation Kit (Roche). Reverse transcription was performed with the iScript cDNA Synthesis Kit (Bio-Rad, Madrid, Spain). Real-time PCR was employed with GoTaq qPCR Master Mix (Promega) in an iCYCLER detection system (Bio-Rad). The amplification profile consisted of an initial denaturation for 5 min at 95 °C and then 40 cycles of 30 s at 95 °C, annealing for 30 s at 60 °C, and elongation for 30 s at 72 °C. A cycle of 10 s at 83 °C and a final extension for 1 min was carried out at 72 °C. Amplification efficiencies were validated and normalized against β-actin, and fold change in gene expression was calculated using the $2^{-\Delta\Delta Ct}$ method. The following primers were used:

HIF-1α-forward: 5′-GAAAGCGCAAGTCTTCAAAG-3′
HIF-1α-reverse: 5′-TGGGTAGGAGATGGAGATGC-3′
SIAH2-forward: 5′-CTATGGAGAAGGTGGCCTCG-3′
SIAH2-reverse: 5′-CGTATGGTGCAGGGTCAGG-3′
HK2-forward: 5′- CAAAGTGACAGTGGGTGTGG-3′
HK2-reverse: 5′- GCCAGGTCCTTCACTGTCTC-3′
BNIP3-forward: 5′-GCTCCCAGACACCACAAGAT-3′
BNIP3-reverse: 5′-TGAGAGTAGCTGTGCGCTTC-3′
HMOX1-forward: 5′-AAGATTGCCCAGAAAGCCCTGGAC-3′
HMOX1-reverse: 5′-AACTGTCGCCACCAGAAAGCTGAG-3′
VEGF-forward: 5′-AGGAGGAGGGCAGAATCATCA-3′
VEGF-reverse: 5′-CTCGATTGGATGGCAGTAGCT-3′
β-actin-forward: 5′-GCTCCTCCTGAGCGCAAG-3′
β-actin-reverse: 5′-CATCTGCTGGAAGGTGGACA-3′

2.7. PCR array

One microgram of RNA was transcribed to cDNA using the RT² First Strand Synthesis Kit (SABiosciences, Frederick, MD, USA) and analyzed using the human hypoxia signaling pathway PCR array (PAHS-032, SABiosciences) and the RT² SYBR green qPCR master mix (330510, SABiosciences). Each array consists of 84 genes involved in hypoxia-related signaling, as well as 12 sequences to control for loading and cDNA quality. The fold change in gene expression was calculated using the $2^{-\Delta\Delta Ct}$ method and five housekeeping genes for normalization following the manufacturer's instructions. Each array was performed in triplicate.

2.8. Angiogenesis assays

HUVECs and HBMECs (2×10^4) were seeded over a uniform layer of Matrigel (BD Biosciences) in a 96-well plate. After 12 h cells were washed with PBS and stained with 5 μM Calcein-AM (Invitrogen, Carlsbad, CA, USA). Tube formation was analyzed using a 4× objective and a BD Pathway 855 Bioimager. Attovision v 1.7 BD software was used to quantify the total length and branch points of tubes.

2.9. Cell viability assay

SK-N-SH cells were seeded in a 96-well plate (7×10^3 per well) for 24 h, pretreated or not with NADA 10 μM for 3 h, and then subjected or not to hypoxia (1% O_2) for 3 h. MTT reagent (5 mg/ml, Sigma-Aldrich) was added and incubated for 3 h at 37 °C in darkness. The formazan crystals were solubilized by the addition of 100 μL DMSO and the absorbance at 550 nm was measured using a Multifunction Microplate Reader (TECAN GENios Pro, Switzerland). All determinations were carried out in triplicate.

2.10. Statistical analysis

Data are expressed as mean ± SD. Differences were analyzed by Student's *t* test. $P < 0.05$ was considered significant. Images were analyzed and quantified using the ImageJ v1.45 software (http://rsbweb.nih.gov/ij/). Statistical analyses were performed using GraphPad Prism version 6.00 (GraphPad, San Diego, CA, USA).

3. Results

3.1. N-acyl-dopamines mediated HIF-1α stabilization through CB_1- and TRPV-1-independent mechanisms

To investigate the effect of several *N*-acyl-dopamines and related compounds on the hypoxia response pathway we determined firstly the steady state levels of HIF-1α protein in neuronal and non-neuronal cell lines. In Fig. 1A it is shown that both NADA and OLDA induced HIF-1α expression at the protein level to the same extent than exposure to low levels of O_2 (1%) in HEK-293T and SK-N-SH cells. In contrast neither AEA nor dopamine was able to induce HIF-1α expression in these cell lines. AM404, a hybrid molecule with CB_1 and TRPV-1 agonistic activities, also failed to induce HIF-1α expression. Using specific chemical antagonists we investigated the involvement of CB_1 and TRPV-1 receptors in NADA-induced HIF-1α expression in SK-N-SH cells. We found that neither AM251 (CB_1 antagonist) nor SB705498 (TRPV-1 antagonist) inhibited the effects of NADA on HIF-1α (Fig. 1B).

N-acyl-dopamines are conjugates of fatty acids with dopamine via an amide bond. To investigate the role of the dopamine moiety in the induction of HIF-1α we treated HEK-293T and SK-N-SH cells with the four endogenous *N*-acyl-dopamines described so far [2,5], namely NADA, OLDA, PALDA and STEARDA. As depicted in Fig. 1C all the *N*-acyl-dopamines analyzed were able to induce HIF-1α expression. Moreover, related endogenous endolipids such as *N*-arachidonoyl-L-tyrosine or synthetic analogs based on hydroxytyrosol, a metabolite of dopamine, such as arachidonoyl hydroxytyrosol ester, oleyl

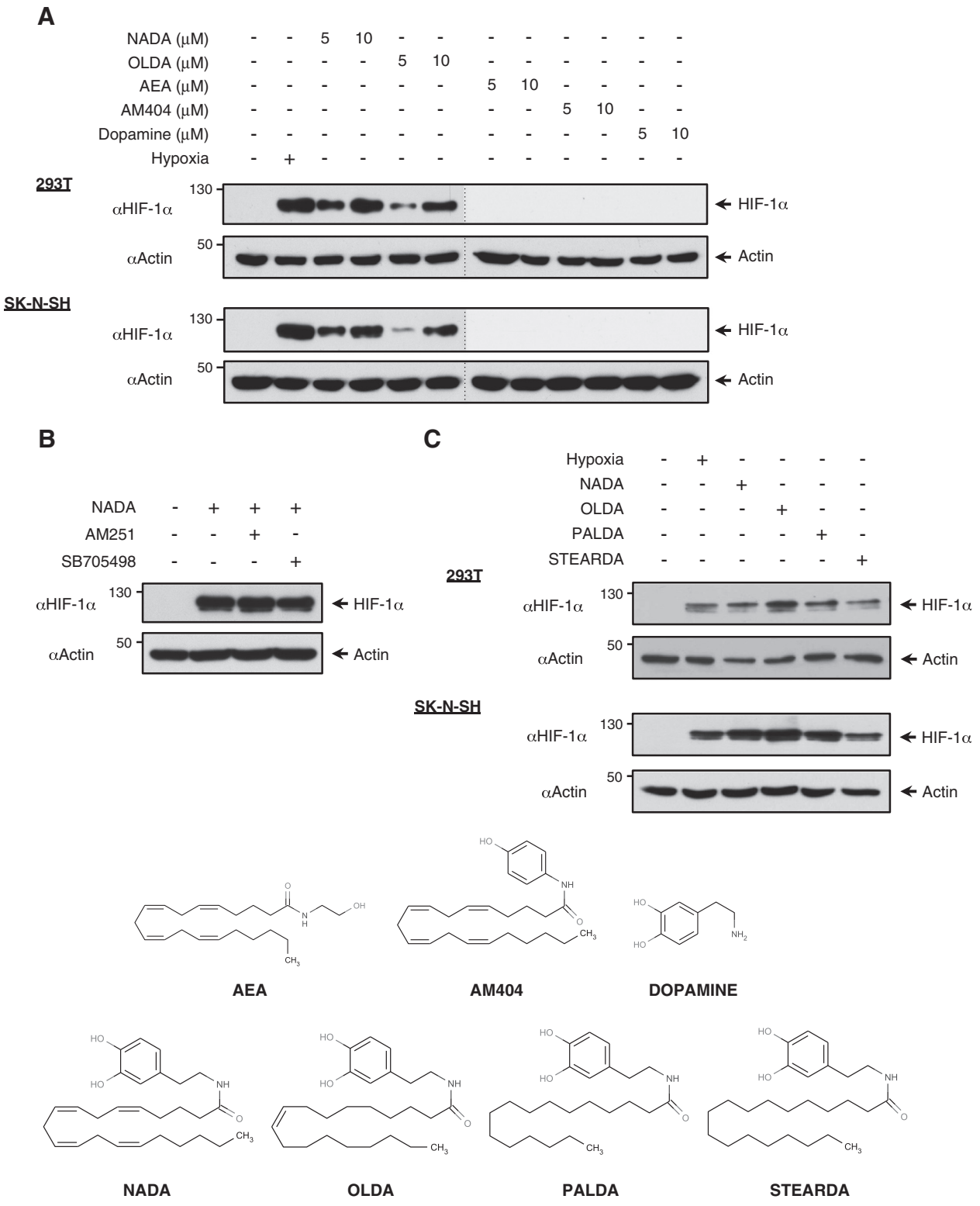

Fig. 1. *N*-acyl-dopamines mediate CB_1/TRPV1-independent HIF-1α stabilization. (A) HEK-293T and SK-N-SH cells were incubated with the different compounds at the indicated doses for 6 h. Hypoxia was induced by the cultivation of cells at 1% O_2 concentrations for 6 h. The expression of HIF-1α protein was determined by immunoblot analysis. (B) SK-N-SH cells were incubated with AM251 (CB_1 antagonist) or SB705498 (TRPV-1 antagonist) for 30 min and stimulated with NADA (10 μM) for 6 h. The expression of HIF-1α protein was determined by immunoblot analysis. We show a representative blot of three independent experiments. (C) Upper panel: cells were treated with the indicated compounds at the same concentration (10 μM) for 6 h and hypoxia was induced as described above. We show a representative blot out of three independent experiments and the positions and molecular weights (in kDa) are indicated. Lower panel: Chemical structures.

hydrotyrosol ester and palmitoyl hydrotyrosol ester failed to induce HIF-1α in SK-N-SH cells (Fig. 2A and B). Altogether these results indicate that the hydroxyl groups of the dopamine moiety are critical for the hypoximimetic activity of *N*-acyl-dopamines.

3.2. NADA stabilizes HIF-1α in different neuronal cell types

To study whether this HIF-1α regulatory mechanism is present in different neuronal cells we analyzed the effect of NADA on MO3.13

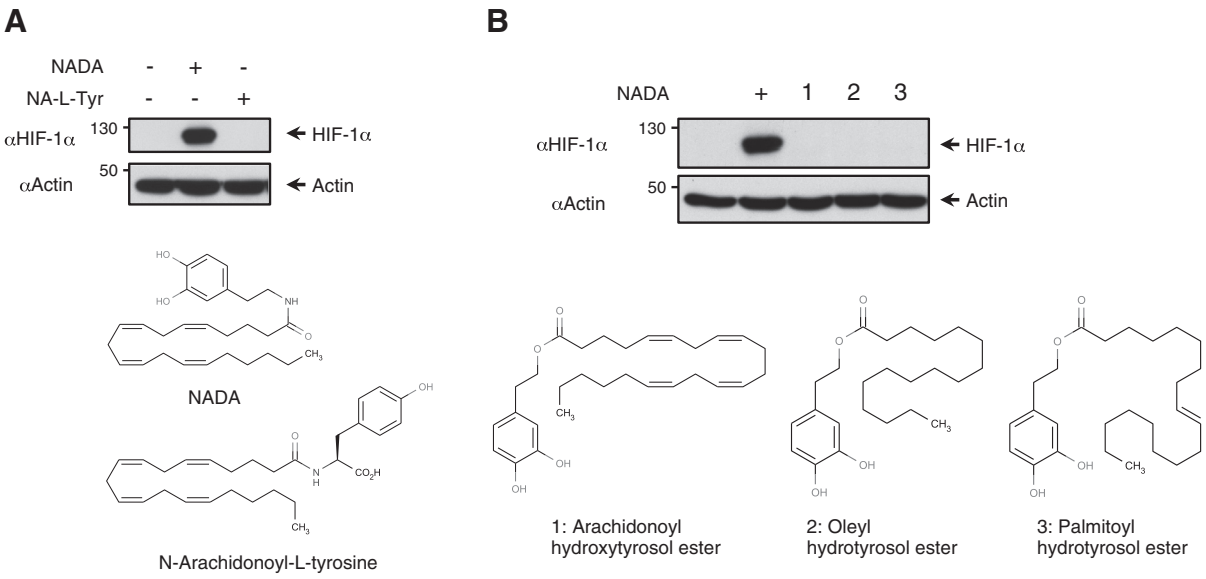

Fig. 2. Hydroxyl groups of the dopamine moiety are critical for the hypoximimetic activity of *N*-acyl-dopamines. (A–B) Upper panel: SK-N-SH cells were treated with the indicated compounds at the same concentration (10 μM) for 6 h and analyzed for HIF-1α expression as shown. We show a representative blot of three independent experiments. Lower panel: Chemical structures.

(oligodendroglial) (Fig. 3A) and U87 (gliobastoma) (Fig. 3B) cell lines. The cells were either subjected to hypoxia (1% O_2) or stimulated with NADA and the levels of HIF-1α detected by immunoblot. In both cell lines NADA induced HIF-1α expression at levels similar to those obtained in response to hypoxia. To further investigate the effect of NADA on primary cells we used human primary astrocytes and neurons. We found that NADA also induced HIF-1α expression in astrocytes (Fig. 3C) and in neurons (Fig. 3D), although in the case of astrocytes the levels were lower than those obtained in response to hypoxia. The differential effect of NADA in the cells analyzed may reflect the singular expression of the specific target(s) for NADA to induce HIF-1α expression.

Next, we investigated the effect of NADA on the HIF-1α expression at the mRNA and protein levels in SK-N-SH cells. As shown in Fig. 3E, NADA stimulation significantly increased HIF-1α expression at the protein level. However, the levels of mRNA for HIF-1α were not significantly changed as revealed by qPCR. Likewise, we monitored HIF-1α protein half-life after NADA and hypoxia treatment in the presence of the protein synthesis inhibitor cycloheximide (CHX). As shown in Fig. 3F, HIF-1α half-life was higher in the NADA treatment compared to the hypoxia condition (22.1 vs 7.9 min). Altogether these results clearly indicate that NADA directly affects HIF-1α stabilization.

3.3. NADA induces degradation of PHD3 and does not synergize with hypoxia to stabilize HIF-1α

To study in detail the HIF-1α regulatory pathway in response to stimulation with *N*-acyl-dopamines, SK-N-SH cells were treated with NADA at the indicated times and the steady state levels of HIF-1α, PHD2 and PHD3 proteins analyzed by immunoblotting. As shown in Fig. 4A (upper panel), NADA caused a clear HIF-1α stabilization after 1 h, had a peak at 3 h and started to decrease after 6 h. The HIF-1α stabilization was accompanied by a gradual decrease in PHD3 levels, without affecting the PHD2 levels. In parallel, to evaluate the effect of HIF-1α stabilization by NADA, SK-N-SH cells were transiently transfected with the HIF-dependent reporter constructs Epo-Luc (containing an HIF-responsive element from the erythropoietin gene) and stimulated in the same conditions described above (Fig. 4A, lower panel). These results clearly indicate that HIF-1α stabilization mediated by NADA is also accompanied by an increase of the transactivation capability of HIF-1α.

Next, we were interested in determining if NADA affected the induction of HIF-1α in cells cultured under hypoxic conditions. SK-N-SH cells were subjected to hypoxia (1% O_2) in the presence or the absence of NADA. We found that NADA causes HIF-1α stabilization with levels similar to those obtained under hypoxia conditions, and the combination of both stimuli produced no significant change (Fig. 4B). Similar to the previous experiment, PHD2 levels were almost unaffected in response to both conditions, whereas PHD3 levels clearly decreased in relation to HIF-1α expression. As expected, the transcriptional activity of HIF-1α on the Epo-Luc reporter was not affected by the treatment of hypoxic cells with NADA (Fig. 4B, lower panel). Collectively, these experiments suggest that HIF-1α stabilization mediated by NADA is conducted through a signaling pathway that is also activated in response to hypoxia without affecting PHD2 expression.

Finally, and knowing HIF-1α stabilization kinetics in response to NADA, we decided to calculate EC50 after 3 h of stimulation (Fig. 4C). Endocannabinoids such as AEA can bind bovine serum albumin and this property could interfere to establish the potency of NADA in cell cultures [44]. Therefore, SK-N-SH cells were grown for 12 h in the presence or absence of FCS and stimulated with different concentrations of NADA. HIF-1α levels were analyzed by western blotting and quantified through densitometry using actin as the housekeeping protein. We found that NADA has an EC50 of 2.6 μM, which was reduced to 2.3 μM after serum withdrawal.

3.4. SIAH2 expression is affected by NADA

To determine the mechanism of action of NADA on hypoxia response pathway, firstly we studied the effect of this *N*-acyl-dopamine on the SIAH2 protein. This ubiquitin ligase controls HIF-1α levels mainly through PHD3 degradation in response to low levels of oxygen (1% to 5% oxygen) [23]. To assess this point, different amounts of SIAH2 were co-expressed with PHD3 in the presence or absence of NADA. As shown in Fig. 5A, SIAH2 expression degraded PHD3 in a dose-dependent manner, whereas HIF-1α levels did not change significantly. Contrary to our expectations, NADA stimulation produced a clear inhibition of SIAH2 expression and therefore we investigated the impact of NADA on the endogenous SIAH2 levels. As shown in Fig. 5B, increasing amounts of NADA resulted in a dose-dependent decrease in SIAH2 protein levels without affecting the gene expression, indicating that the effect of NADA on SIAH2 expression relied at the protein level. To further

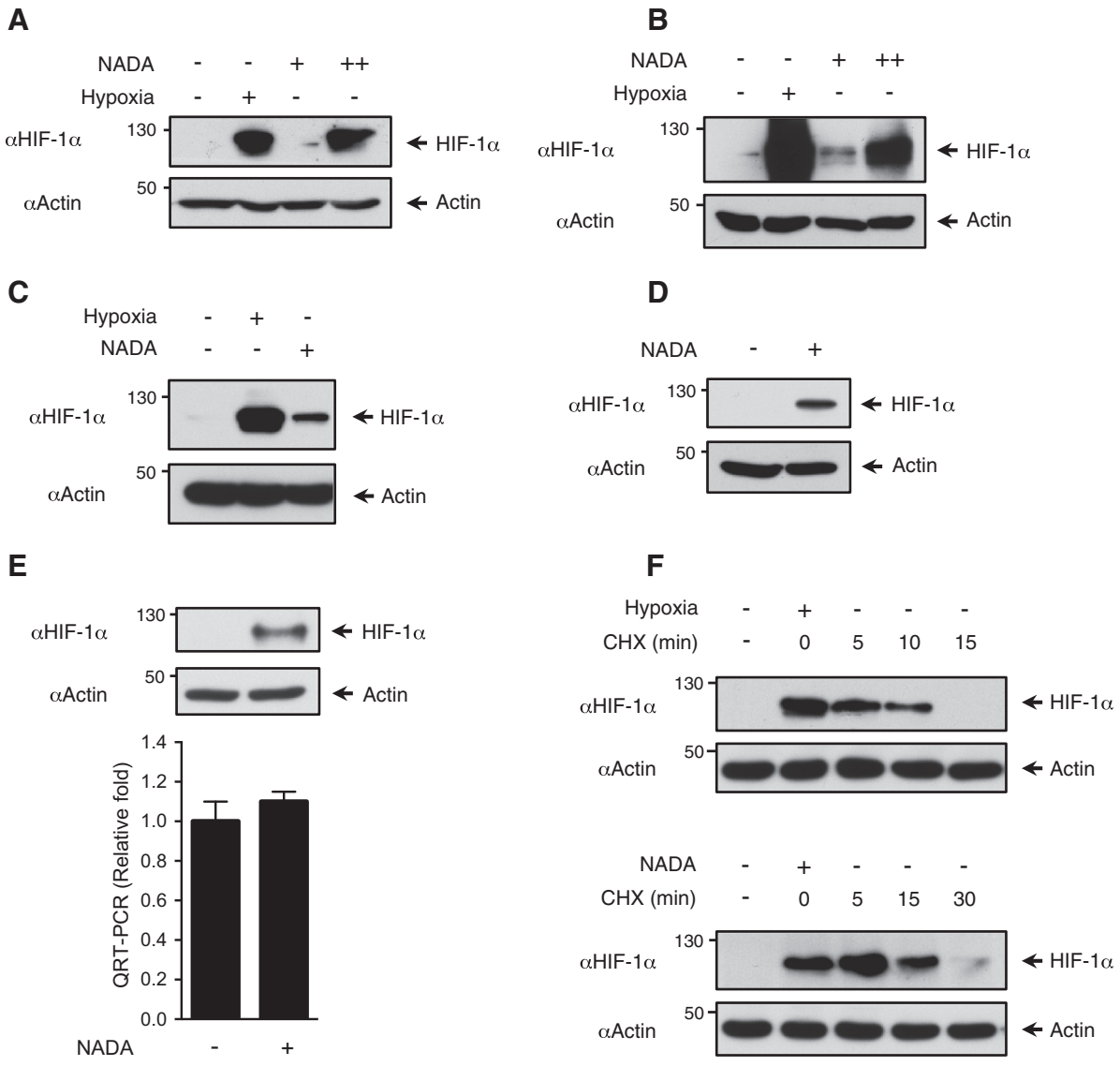

Fig. 3. NADA stabilizes HIF-1α in different neuronal cells. MO3.13 (A) and U87 (B) cells were either subjected to hypoxia (1% O_2) or stimulated with NADA (+, 1 μM; ++, 10 μM) for 6 h and analyzed for HIF-1α expression as shown. (C) Human primary astrocytes were either subjected to hypoxia (1% O_2) or stimulated with NADA (10 μM) for 6 h. HIF-1α expression was analyzed by immunoblotting with the indicated antibody. (D) Human primary neurons were incubated for 6 h with NADA (10 μM). The expression of HIF-1α protein was determined by immunoblot analysis. We show a representative blot out of three independent experiments. (E) SK-N-SH cells were stimulated with NADA (10 μM) for 6 h, lysed and further analyzed for HIF-1α protein expression by immunoblots (upper panel) and mRNA expression by qPCR (lower panel). Data are mean ± SD of n = 3 experiments. (F) SK-N-SH cells were either subjected to hypoxia (1% O_2) or stimulated with NADA (10 μM) for 6 h, washed twice with PBS and treated with the protein synthesis inhibitor cycloheximide (CHX) (40 μg/ml) for the indicated time. HIF-1α expression was analyzed by immunoblotting using actin expression as the loading control. We show a representative blot out of three independent experiments.

investigate this possibility we expressed SIAH2 and the cells were treated with NADA in the presence or absence of the proteasome inhibitor MG-132. We found that NADA strongly inhibited SIAH2 expression and this effect was almost completely abolished in the presence of MG-132. Altogether our data indicate that NADA-mediated SIAH2 degradation is performed by the proteasome (Fig. 5C).

To demonstrate the contribution of SIAH2 in NADA-induced HIF-1α stabilization, we knocked down SIAH2 by siRNA treatment. As shown in Fig. 5D (and Supplementary Fig. 1), SIAH2 silencing drastically reduced the expression of HIF-1α in response to NADA treatment. Similarly, inhibition of SIAH2 expression induced stabilization of PHD3 in response to NADA. A comparison of MEFs lacking Siah1a/2 revealed that NADA-induced PHD3 degradation was more prominent in wild type cells (Fig. 5E). Finally, and to confirm the role of PHD3 on HIF-1α stabilization in response to NADA, we over-expressed PHD3 and analyzed the effect of NADA on endogenous HIF-1α expression. As shown in Fig. 5F, transfection of PHD3 decreased NADA-induced stabilization of HIF-1α, suggesting that the abundance of PHD3 is determinant to mediate NADA-induced HIF-1α stabilization. Collectively, these experiments showed that SIAH2 and PHD3 play a relevant role, but not exclusively, in NADA-induced HIF-1α stabilization. However other proteins with function similar to SIAH1 and PHD1 could also exhibit functional redundancy in this process.

3.5. NADA increases SIAH2 activity and decreases SIAH2 protein level

Are *N*-acyl-dopamines affecting SIAH2 activity? One of the main characteristics of RING domain E3 ubiquitin ligases is their ability to limit their own availability through self-ubiquitination and degradation [39]. The capacity of NADA to inhibit the expression of both SIAH2 and its substrate PHD3 (Fig. 5A) led us to consider the possibility that this *N*-acyl-dopamine is increasing the E3 ligase activity of SIAH2, and therefore its own degradation. To test this hypothesis, first we analyzed the effect of NADA on a SIAH2 point ligase-deficient mutant (SIAH2 RM,

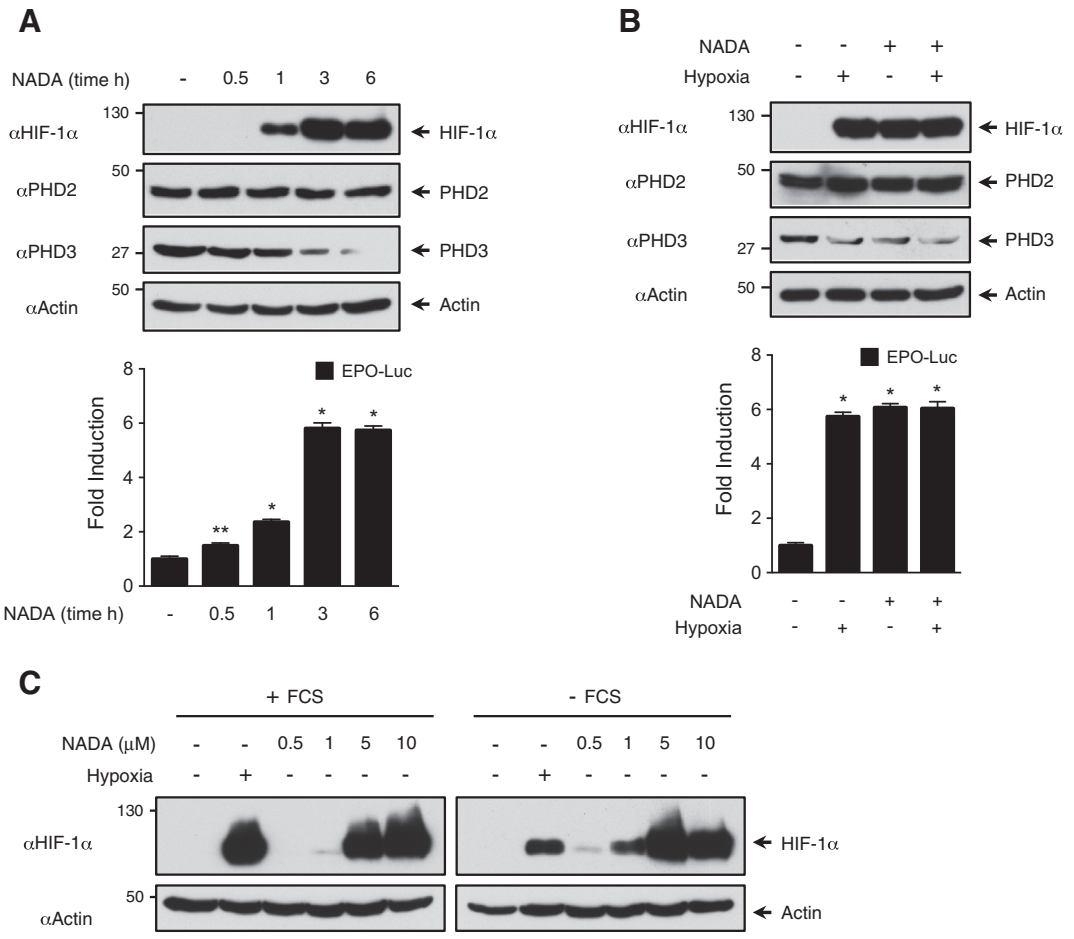

Fig. 4. NADA does not synergize with Hypoxia. (A) SK-N-SH cells were transfected with a HIF-1α-responsive vector, and erythropoietin promoter-controlled luciferase construct (Epo-Luc). Twenty-four hours later, cells were stimulated with NADA (10 μM) at the indicated times, lysed and further analyzed for HIF-1α, PHD2 and PHD3 expression by immunoblots (upper panel) and luciferase expression (upper panel). Data are mean ± SD of n = 3 experiments. $^{*}P = 0.0039$, $^{**}P < 0.0001$. (B) SK-N-SH cells were transfected with Epo-Luc vector and 48 h later were either subjected to hypoxia (1% O_2) or/and stimulated with NADA (10 μM) for 6 h. Cells were harvested and one aliquot was analyzed for the levels of the HIF-1α, PHD2 and PHD3 proteins by immunoblots while another aliquot was used to study luciferase expression. Data are mean ± SD of n = 3 experiments. $^{*}P < 0.0001$. (C) SK-N-SH cells were grown in medium with or without FCS (fetal calf serum) for 12 h and were either subjected to hypoxia (1% O_2) for 6 h or stimulated with NADA at the indicated concentration for 3 h. HIF-1α expression was analyzed by immunoblotting with the indicated antibody. We show a representative blot out of three independent experiments.

Ring Mutant, H98A/C101A). As shown in Fig. 6A, NADA did not affect the stability of SIAH2 RM in the absence or presence of MG-132 and similarly to the previous results, NADA induced HIF-1α stabilization. These findings support the hypothesis that NADA can affect SIAH2 self-degradation, since its effect depends on intact RING domain.

To determine whether NADA altered SIAH2 stability, we monitored SIAH2 half-life in the presence of cycloheximide (CHX). As shown in Fig. 6B, HEK-293T cells stimulated with NADA reduced the half-life of SIAH2 protein from 6 to 3 h. However, no significant change was observed in the case of SIAH2 RM. All these data suggest that NADA ability to reduce SIAH2 stability is due to its ability to increase the E3 ligase activity of SIAH2. To demonstrate that NADA increases SIAH2 activity by affecting its auto-ubiquitination, we decided to compare the SIAH2 ubiquitination levels in the presence or absence of NADA. We co-expressed HA-Ubiquitin and Flag-SIAH2 with or without NADA in the presence of MG-132, and analyzed the ubiquitination status of SIAH2 after immunoprecipitation and immunoblotting. These experiments showed that NADA strongly stimulated basal SIAH2 polyubiquitination (Fig. 6C), and demonstrated that NADA increased SIAH2 activity.

We next undertook experiments designed to determine how NADA affects SIAH2 protein regulation. Firstly, we explored the possibility that NADA could be altering the SIAH2 dimerization, one of the key regulatory mechanisms that control its catalytic activities. Co-expression of Flag-SIAH2 and HA-SIAH2 in HEK-293T cells showed strong interaction in the presence and absence of NADA (Fig. 7A). No differences were observed between the SIAH2 expression after the immunoprecipitation in the presence of NADA and the input levels, indicating that SIAH2 dimerization is not affected. Similar results were obtained using the SIAH2-RM mutant (Fig. 7B). Secondly, since it has been previously described that the PI3K/AKT pathway mediated the regulation of SIAH2 expression [45], we analyzed the possible role of this pathway on NADA-induced HIF-1α expression. To this end, the cells were stimulated with NADA in the absence and the presence of a LY 294002, a PI3K inhibitor, and the expression of phospho-AKT and HIF-1α determined by immunoblots. We found that NADA slightly increased AKT phosphorylation but HIF-1α expression was not affected in the presence of LY 294002 (Fig. 7C), which indicates that the AKT pathway is not involved in this process.

Next, we asked whether the SIAH2 phosphorylation level, the best-described mechanisms responsible for regulating SIAH2 activity, was involved in this process. Several protein kinases able to phosphorylate SIAH2 in different residues modifying their activity have been described [29,35,40]. We study the ability of NADA to alter SIAH2 wild type stability compared with the SIAH2 mutants where all the phosphorylation sites described have been either mutated to alanine (SIAH2-5A; Ser16, Thr26, Ser28, Ser68, and Thr119) or in a phosphorylation-mimicking fashion to aspartic acid (SIAH2-5D). HEK-293T cells were transfected with Flag-SIAH2-WT, Flag-SIAH2-5A, and Flag-SIAH2-5D and treated with NADA. We found that SIAH2 stability in all the cases was inhibited by NADA to a similar extent (Fig. 7D). Similarly, NADA did not affect the

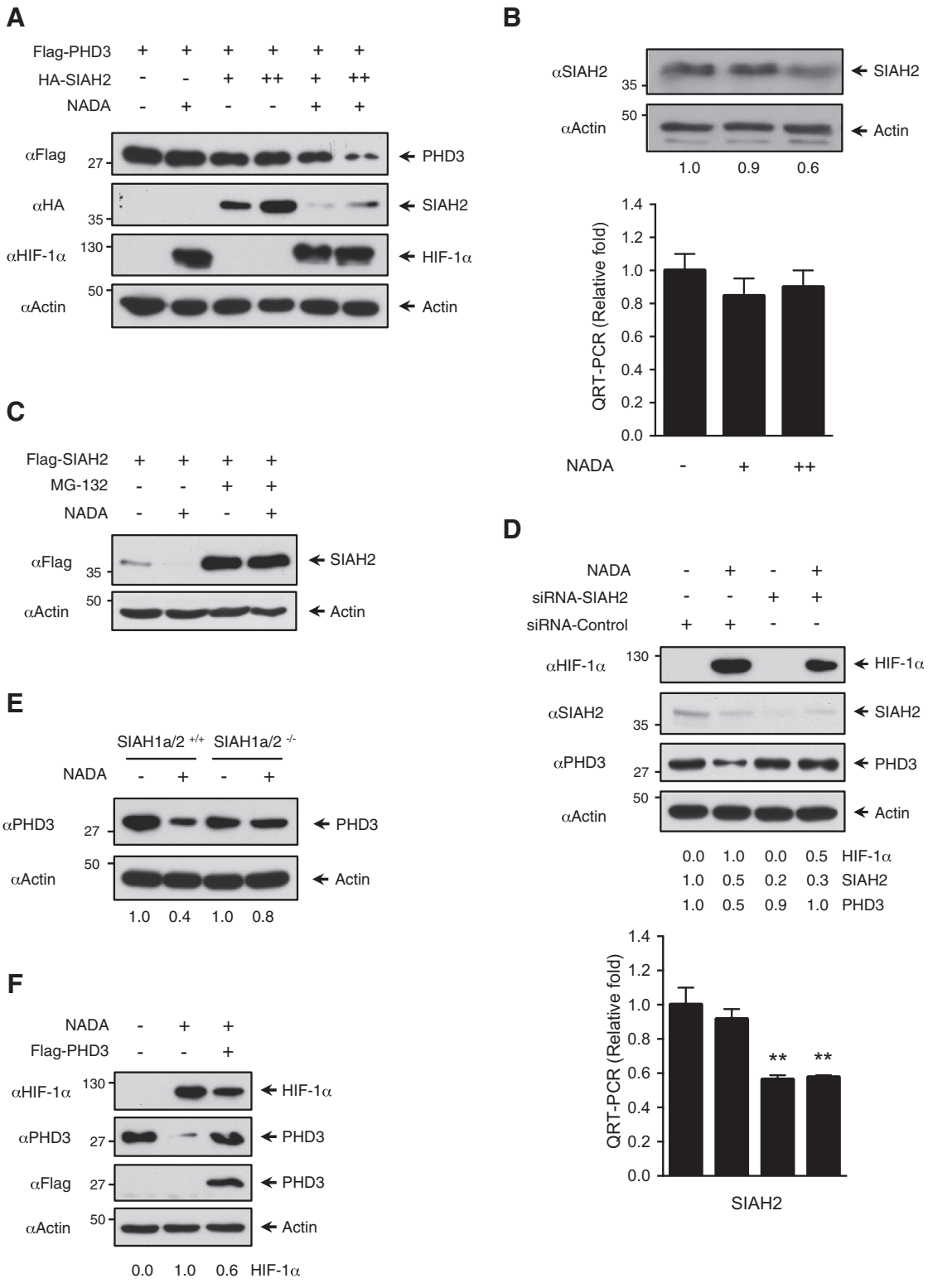

Fig. 5. SIAH2 expression is affected by NADA. (A) HEK-293T cells were transfected with the indicated plasmids to express Flag-PHD3 and different amounts of SIAH2. After 36 h, NADA (10 μM) was added for another 6 h. Cells were lysed and protein expression was evaluated by immunoblot with the indicated antibodies. (B) HEK-293T cells were stimulated with NADA (+, 1 μM; ++, 10 μM) for 10 h, and harvested and one aliquot was analyzed for the levels of the SIAH protein by immunoblot (upper panel) while another aliquot was analyzed by qPCR to measure SIAH2 mRNA levels (lower panel). Data are mean ± SD of n = 3 experiments. The values below the gels indicate SIAH2 protein signal intensities (quantified using ImageJ) after normalization to actin signal intensities. (C) HEK-293T cells were transfected to express Flag-SIAH2 and stimulated with NADA (10 μM) in the presence or absence of 10 μM of MG-132 as shown. Cell lysates were analyzed by immunoblot with the indicated antibodies. (D) HEK-293T cells were transfected with 100 nM of SIAH2 or scrambled (control) siRNAs. After 4 days, cells were stimulated with NADA (10 μM) for 10 h, and lysed and one aliquot was analyzed for the levels of endogenous protein expression by immunoblot with the indicated antibodies (upper panel, one representative experiment out of three replicates is shown. Supplementary Fig. 1) while another aliquot was analyzed by qPCR to measure SIAH2 mRNA levels (lower panel). Data are mean ± SD of n = 3 experiments. $^{**}P < 0.001$. The values below the gels indicate SIAH2, PHD3 and HIF-1α protein signal intensities (quantified using ImageJ) after normalization to actin signal intensities. (E) Knockout MEFs lacking Siah1a and Siah2 genes and wildtype controls were treated for 6 h with NADA (10 μM), and lysed and PHD3 endogenous protein expression was evaluated by immunoblot using actin expression as the loading control. The values below the gels indicate PHD3 protein signal intensities (quantified using ImageJ) after normalization to actin signal intensities. (F) HEK-293T cells were transfected with Flag-PHD3 to obtain a similar PHD3 level to endogenous after 6 h of stimulation with NADA (10 μM). Cells were lysed and protein expression was evaluated by immunoblot with the indicated antibodies. The values below the gels indicate HIF-1α protein signal intensities (quantified using ImageJ) after normalization to actin signal intensities.

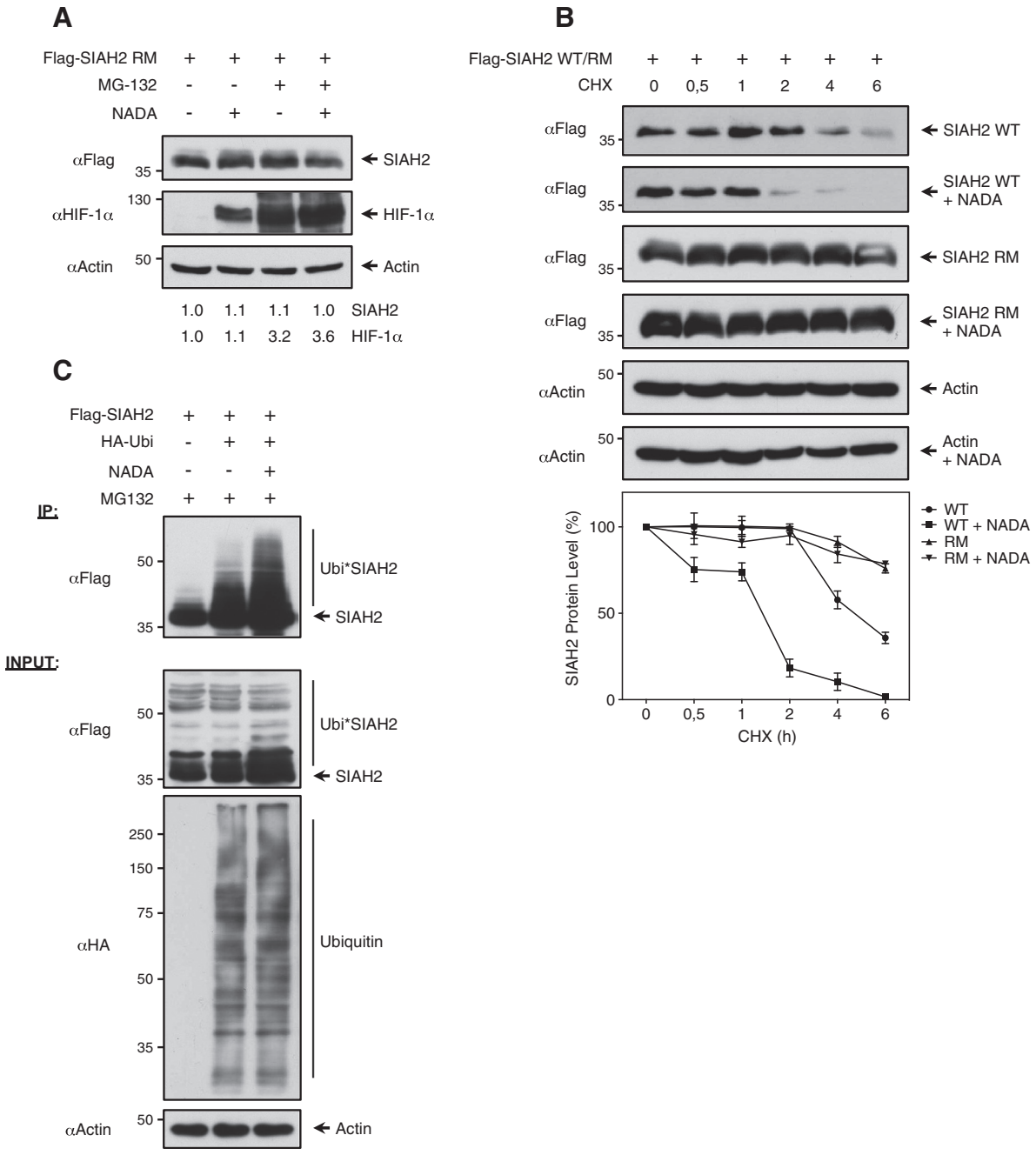

Fig. 6. NADA increases SIAH2 activity and decreases SIAH2 protein expression. (A) HEK-293T cell were transfected to express SIAH2 Ring Mutant (RM) and after 36 h were stimulated with NADA (10 μM) in the presence or absence of MG-132. After 10 h, cells were lysed and SIAH2 and HIF-1α protein expression was analyzed by immunoblot. The values below the gels indicate SIAH2 and HIF-1α protein signal intensities (quantified using ImageJ) after normalization to actin signal intensities. (B) HEK-293T cells were transfected with FLAG-SIAH2 wild-type (WT) or SIAH2 Ring Mutant (RM) and treated with the protein synthesis inhibitor cycloheximide (CHX) (40 μg/ml) for 0.5, 1, 2, 4, and 6 h in the presence or absence of NADA (10 μM). Cell lysates were analyzed by immunoblot using actin expression as the loading control. The graph represents the mean ± SD of band density from 3 different experiments. (C) HEK-293T cells were transfected with Flag-SIAH2, and HA-tagged ubiquitin and 36 h later stimulated with NADA (10 μM) in the presence of MG-132. A fraction of the extract was analyzed by western blotting for the occurrence and ubiquitination of SIAH2 (INPUT, lower panel). Another aliquot was lysed and subjected to immunoprecipitation (IP, upper panel) using anti-Flag antibody. After elution the Flag-SIAH2 protein was detected by western blotting. The position of ubiquitinated SIAH2 is indicated.

SIAH2 phosphorylation levels mediated by HIPK2 (Fig. 7E). Moreover, NADA induced a clear inhibition in the expression of both over-expressed and endogenous HIPK2 and DYRK2 proteins (SIAH2-specific substrates) (Fig. 7F and G). All these results indicate that SIAH2 phosphorylation is not involved in the mechanism of action of NADA.

3.6. NADA increases the expression of neuroprotective genes and angiogenesis

To determine the consequences of HIF-1α stabilization mediated by NADA, next we decided to study its effect on gene expression. Human primary astrocytes were stimulated with NADA (10 μM for 6 h) and mRNA levels of 84 genes involved in the hypoxia response pathway were studied through qPCR array analysis (Fig. 8A). From the analyzed genes, 18 showed changes when compared with the normoxic situation (Table 1). Interestingly, HIF-1α target genes such as HMOX1, HK2, VEGFA and BNIP3 are related with cell survival and neuroprotection and were upregulated by NADA in primary astrocytes.

Next we analyzed in detail the expression of selected genes by qRT-PCR, to determine if NADA affected their induction in human primary astrocyte cells cultured under hypoxic conditions. As shown in Fig. 8B,

NADA induced the expression of HMOX1, HK2 and BNIP3 to levels similar to those obtained under hypoxia conditions, and the combination of both stimuli produced no significant changes. In contrast, we observed a synergy of both stimuli in the case of VEGFA expression.

To further evaluate *N*-acyl-dopamines' capacity to induce cell survival in response to hypoxia, we decided to investigate the potential cytoprotective effect of NADA in response to hypoxia in an in vitro model of hypoxia-induced cell death [46,47]. SK-N-SH cells were pretreated or not with NADA for 3 h and then subjected to hypoxia for 3 more hours. As shown in Fig. 8C, NADA alone did not affect cell viability but significantly ($P = 0.0036$) protected the cells from hypoxia-induced cytotoxicity. Finally, to test the functional consequences of

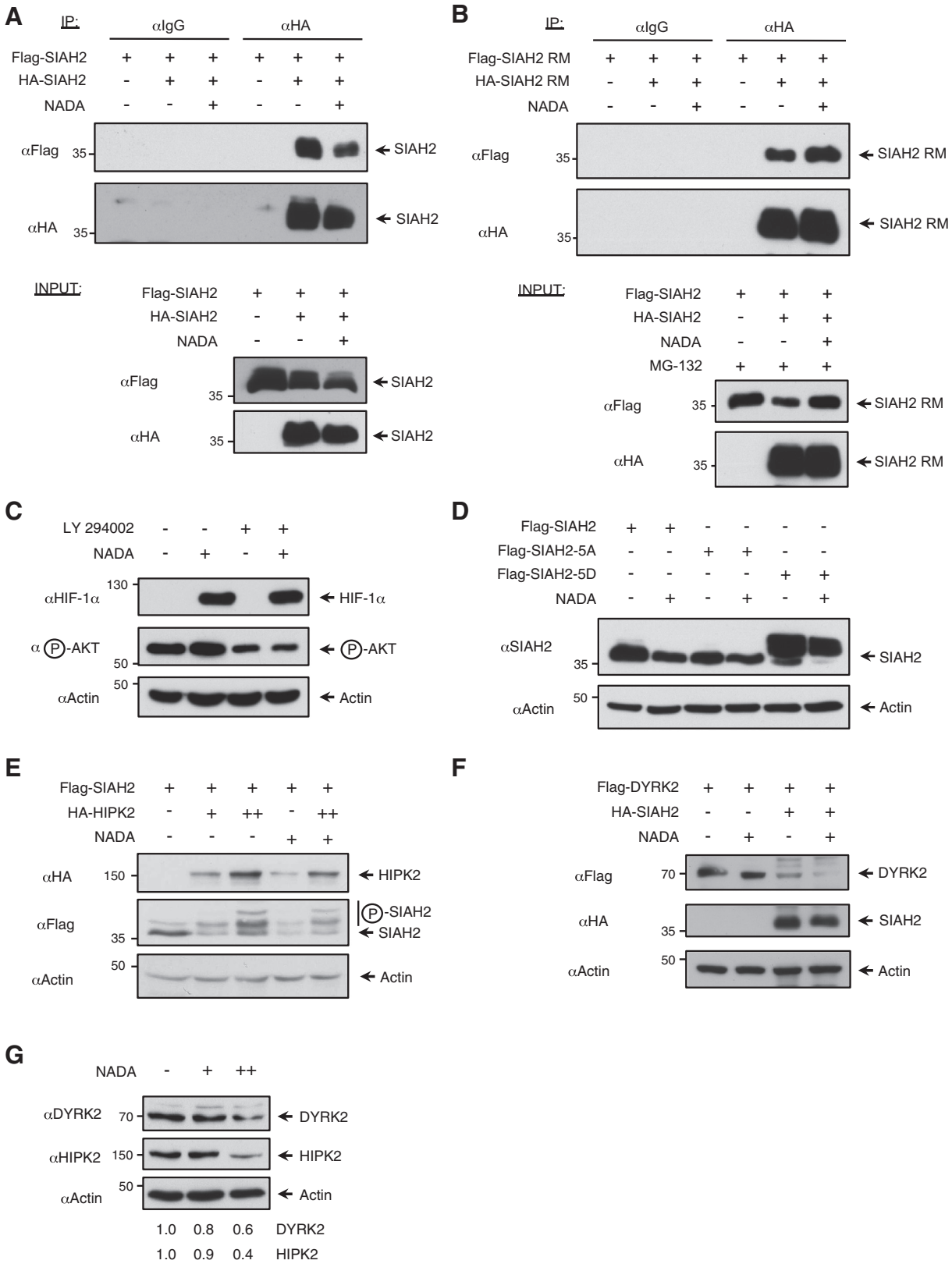

NADA stimulation in a physiological model, we measured endothelial cell tube formation as a model of angiogenesis. Human umbilical vein endothelial cells (HUVECs; Fig. 8D) and human brain microvascular endothelial cells (HBMECs; Fig. 8E) were stimulated with NADA (10 μM) for 6 h and tube formation was quantified using a BD Pathway TM Bioimager. NADA stimulation resulted in an increase in the branch points of tubes in HUVEC and HBMEC and in an increase in the total length of tubes in HUVEC but not in HBMEC.

4. Discussion

Neuronal damage secondary to brain injuries such as cerebral hypoxia and neurodegenerative process, is a complex process that involves inflammatory changes. The activation of a common mechanism related to survival or cell death, mediated by the stabilization and transactivation of HIF-1α, has been observed in these conditions. PHDs are the gatekeepers for the oxygen-dependent degradation of HIF-1α and also function as integrated sensors of cellular metabolism [48]. The phenomenon that hypoxic preconditioning (HP) protects against subsequent severe anoxia was discovered approximately two decades ago, and subsequently has been demonstrated in different hypoxic model systems [15]. Therefore PHD inhibition by hypoximimetic small-molecules represents an interesting strategy or the development of neuroprotective therapies and for prevention against hypoxic conditions [15].

We previously described that NADA and OLDA also inhibit NF-κB by targeting the phosphorylation of p65/RelA [9]. Although the role of NF-κB in neuroprotection has been controversial, it has been shown that NF-κB inhibition results in neuroprotection in different experimental models. Microglial NF-κB activation has been proposed to promote brain damage via induction of pro-inflammatory cytokines [49]. In addition, strong evidence indicates that NF-κB activation in neurons contributes to ischemia-induced neuronal injury [49]. Thus, *N*-acyl-dopamines may exert neuroprotective activity through pleiotropic mechanisms that include at least HIF-1α induction, NF-κB inhibition and CB_1 activation.

What is the mechanism responsible for the observed effect of *N*-acyl-dopamines in this study? Different conditions able to modify the levels and activity of SIAH family proteins, including glucose level changes, DNA damage, apoptosis and hypoxia have been described [23,50–53]. In the literature there are only a few data about the regulation capacity of SIAH2 at a transcriptional level in response to these stimuli [36,37,54]. However, there is an abundance of mechanisms mediated through post-translational modifications. It has been described that activation of the AKT pathway can increase transcription levels of SIAH2, modulating hypoxic signaling through PHD3 degradation and HIF-1α stabilization [45]. Experiments of HIF-1α stabilization in response to NADA were not affected in the presence of the PI3K/Akt inhibitor LY 294002. These results, together with the lack of effects observed in SIAH2 transcription, seem to rule out a possible role of NADA on this pathway.

Among the post-translational modifications described to date which are able to regulate SIAH2, the capacity to self-ubiquitinate under normal physiological conditions to limit its availability and activity stands out [55]. This ability is regulated by other post-translational SIAH2 modifications, such as the phosphorylation performed by different protein kinases in response to several stimuli [29,35], as well as by the action of select deubiquitinating enzymes [56]. Others and we have described the kinases able to phosphorylate SIAH2, such as p38, HIPK2 and DYRK2, affecting the residues serines 16, 28 and 69 and threonines 26 and 119 [29,40,57]. In this study we have analyzed in detail how the presence of NADA directly affects SIAH2 phosphorylation and activity mediated by DYRK2 and HIPK2. Similarly, we have analyzed the effect of NADA on different mutants where all the phosphorylation sites described to date have been mutated either to alanine or in a phosphorylation-mimicking fashion to aspartic acid. We found that SIAH2 phosphorylation and stability levels were altered by NADA in a similar way in all cases. Altogether, these data seem to indicate that SIAH2 phosphorylation in these residues is not involved in the NADA action mechanism. However, we cannot rule out the possibility that NADA could target an unidentified upstream kinase able to phosphorylate and modify SIAH2. Likewise, we cannot discard that NADA may exert its effect through the alteration of another post-translational regulation mechanism which could enhance SIAH2 activity.

Another mechanism we considered was the possible direct interaction between *N*-acyl-dopamines and SIAH2. Until nowadays menadione (Vitamin K3) is the only described compound able to inhibit SIAH2 activity, which is possibly due to a direct effect on its conformation [42]. In the case of the opposing effect exerted by NADA, although we have not experimentally ruled out a direct interaction, it does not seem probable in the light of our results. The inability of NADA to alter the interaction between SIAH2 dimers, as well as its lack of effect on SIAH2 interaction with some of its substrates (data not shown), seems to discard this possibility.

Since the concentrations of NADA in normal and pathological conditions are unknown, it is difficult to speculate about the physiological relevance of our findings. However, the relatively high concentrations of NADA (EC50: 2.6 μM) required for HIF-1α induction should not be seen as evidence against a physiological role for this *N*-acyl-dopamine. NADA was detected in the rat striatum at nanomolar concentrations but it has been described that NADA is short-lived and thus difficult to measure [2,8,58]. It is well known that endocannabinoids, and perhaps other neurolipids, are produced upon demand and are rapidly degraded. Therefore the cellular levels of endocannabinoids may be higher than those found in tissues. For instance, Biswas et al. have shown that AEA could reach up to 50 μM inside the cells at the site of inflammation [59]. In addition, it has been shown that the so called "entourage effect" of endocannabinoids may lower the concentrations of *N*-acyl-dopamines required for a specific biological effect. Moreover NADA may bind to the albumin present in the fetal bovine serum and we have found that the concentrations of NADA required to induce HIF-1α expression are sensibly lower in experiments performed in serum-free media.

Although the biosynthesis and catabolism of NADA is not completely understood, it has been suggested that fatty acid amide hydrolase (FAAH) and tyrosine hydroxylase mediate NADA biosynthesis and catechol-*O*-methyl transferase (COMT) regulates its catabolism [58]. However, it has been found that in hepatic stellate cells FAAH plays a role in NADA degradation rather than in NADA synthesis [8]. In addition, sulfation of *N*-acyl-dopamines in rat liver and nervous system by

Fig. 7. SIAH2 phosphorylation is not affected by NADA. (A–B) HEK-293T cells were transfected with Flag-SIAH2 and HA-SIAH2 (or SIAH2 Ring Mutant, RM) treated with 10 μM NADA for 10 h before lysis. A fraction was subjected to immunoprecipitation (IP) using anti-HA antibody. After elution Flag-SIAH2 protein was detected by western blotting. The remaining extract fraction was tested for the occurrence of the indicated proteins by immunoblot (INPUT). (C) HEK-293T cells were incubated with PI3K inhibitor LY 294002 (10 μM) 30 min before stimulation with NADA (10 μM) for 6 h before lysis. Protein expression was evaluated by immunoblotting with the indicated antibodies. (D) HEK-293T cells were transfected with expression vectors encoding Flag-SIAH2 and the variant mutants Flag-SIAH2-5A and Flag-SIAH2-5D. After 36 h, cells were stimulated with NADA (10 μM) for 10 h, lysed and protein expression evaluated by immunoblot with the indicated antibodies. (E) HEK-293T cells were transfected with the indicated plasmids, and after 36 h treated with 10 μM NADA for 10 h, and lysed and protein expression was evaluated by immunoblot with the indicated antibodies. SIAH2 phosphorylation was seen by the upshifted band. The positions and molecular weights (in kDa) are indicated. (F) HEK-293T cells were transfected with the indicated plasmids, and after 36 h treated with 10 μM NADA for 10 h, lysed and protein expression was evaluated by immunoblot with the indicated antibodies. (G) MO3.13 cells were stimulated with NADA (+, 1 μM; ++, 10 μM) for 6 h and analyzed for HIPK2 and DYRK2 expression as shown. We show a representative blot out of three independent experiments. The values below the gels indicate DYRK2 and HIPK2 protein signal intensities (quantified using ImageJ) after normalization to actin signal intensities.

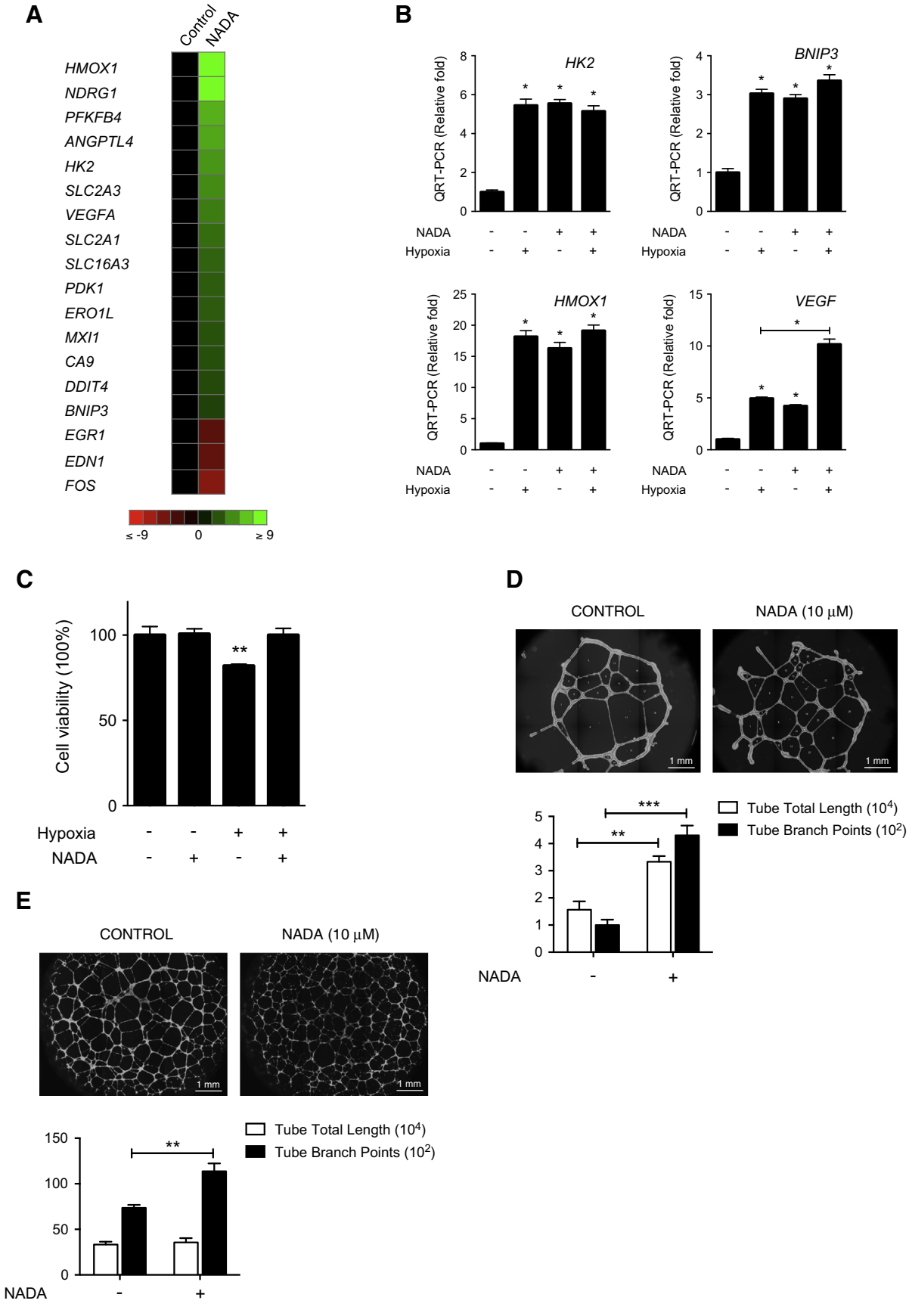
A
Control
NADA
HMOX1
NDRG1
PFKFB4
ANGPTL4
HK2
SLC2A3
VEGFA
SLC2A1
SLC16A3
PDK1
ERO1L
MXI1
CA9
DDIT4
BNIP3
EGR1
EDN1
FOS
≤ -9
0
≥ 9
B
HK2
BNIP3
HMOX1
VEGF
QRT-PCR (Relative fold)
NADA
Hypoxia
C
Cell viability (100%)
Hypoxia
NADA
D
CONTROL
NADA (10 μM)
1 mm
Tube Total Length (10^4)
Tube Branch Points (10^2)
E
CONTROL
NADA (10 μM)
1 mm
Tube Total Length (10^4)
Tube Branch Points (10^2)
NADA

Table 1
Genes involved in the hypoxia response pathway altered by NADA stimulation.

Gene	Name	Fold induction
HMOX1	Heme oxygenase (decycling) 1	28.09
NDRG1	N-myc downstream regulated 1	25.67
PFKFB4	6-Phosphofructo-2-kinase/fructose-2,6-biphosphatase 4	6.60
ANGPTL4	Angiopoietin-like 4	6.33
HK2	Hexokinase 2	5.74
SLC2A3	Solute carrier family 2 (facilitated glucose transporter), member 3	5.43
VEGFA	Vascular endothelial growth factor A	4.97
SLC2A1	Solute carrier family 2 (facilitated glucose transporter), member 1	4.48
SLC16A3	Solute carrier family 16, member 3 (monocarboxylic acid transporter 4)	4.15
PDK1	Pyruvate dehydrogenase kinase, isozyme 1	3.98
ERO1L	ERO1-like (S. cerevisiae)	3.90
MXI1	MAX interactor 1	3.64
CA9	Carbonic anhydrase IX	3.54
DDIT4	DNA-damage-inducible transcript 4	3.34
BNIP3	BCL2/adenovirus E1B 19 kDa interacting protein 3	3.08
EGR1	Early growth response 1	−3.27
EDN1	Endothelin 1	−3.65
FOS	FBJ murine osteosarcoma viral oncogene homolog	−5.34

arylsulfotrasnferases (ASTs) has been investigated as the putative catabolic pathway for those endolipids, also suggesting that their catabolism may be different in distinct tissues [60]. Since we have identified specific genes upregulated by NADA in primary astrocytes we are currently investigating in vivo if the treatment with FAAH, COMT or AST inhibitors can induce the expression of such genes with the aim of validating surrogated markers for the action of *N*-acyl-dopamines in brain and liver.

In summary, this study offers a new mechanism of action for *N*-acyl-dopamines with important consequences on the hypoxia response and the control of angiogenesis in a neuronal context. We demonstrate how NADA can modulate SIAH2 activity, affecting the stability of some substrates including PHD3, HIPK2 and DYRK2. PHD3 inhibition affects the expression of the transcription factor HIF-1α, which promoted the expression of genes such as EPO, VEGFA, HMOX1, HK2 and BNIP3 that are involved in angiogenesis, neuroprotection and cell survival. The potential pharmacological modulation of *N*-acyl-dopamines opens the door to the development of new therapies with important implications in the prevention of processes such as brain ischemia and neurodegenerative disorders.

Supplementary data to this article can be found online at http://dx.doi.org/10.1016/j.bbamcr.2014.07.005.

Authors'contributions

RS, ML and VG performed the experiments and collect data; MAC and EM designed the study, wrote the manuscript and approved the final version to be published. All authors read and approved the final manuscript.

Acknowledgements

We thank Dr. David Bowtell and Dr. Andreas Möller for SIAH knockout MEFs and Dr. M. L. Schmitz for the anti-HIPK2 antibody. This work was supported by MICINN (SAF2010-17122) and Consejería de Salud (Junta de Andalucía) (PI-0650-2010 and PI-0246-2013) grants to M.A.C., and by MICINN (SAF2010-19292) and Junta de Andalucía (P09-CTS-4973) grants to E.M. Finally, we acknowledge Carmen Cabrero-Doncel for her assistance with the article.

References

[1] M. Connor, C.W. Vaughan, R.J. Vandenberg, N-acyl amino acids and N-acyl neurotransmitter conjugates: neuromodulators and probes for new drug targets, Br. J. Pharmacol. 160 (2010) 1857–1871.
[2] S.M. Huang, T. Bisogno, M. Trevisani, A. Al-Hayani, L. De Petrocellis, F. Fezza, M. Tognetto, T.J. Petros, J.F. Krey, C.J. Chu, J.D. Miller, S.N. Davies, P. Geppetti, J.M. Walker, V. Di Marzo, An endogenous capsaicin-like substance with high potency at recombinant and native vanilloid VR1 receptors, Proc. Natl. Acad. Sci. U. S. A. 99 (2002) 8400–8405.
[3] A. Toth, N. Kedei, Y. Wang, P.M. Blumberg, Arachidonyl dopamine as a ligand for the vanilloid receptor VR1 of the rat, Life Sci. 73 (2003) 487–498.
[4] T. Bisogno, D. Melck, M. Bobrov, N.M. Gretskaya, V.V. Bezuglov, L. De Petrocellis, V. Di Marzo, N-acyl-dopamines: novel synthetic CB(1) cannabinoid-receptor ligands and inhibitors of anandamide inactivation with cannabimimetic activity in vitro and in vivo, Biochem. J. 351 (Pt 3) (2000) 817–824.
[5] C.J. Chu, S.M. Huang, L. De Petrocellis, T. Bisogno, S.A. Ewing, J.D. Miller, R.E. Zipkin, N. Daddario, G. Appendino, V. Di Marzo, J.M. Walker, N-oleoyldopamine, a novel endogenous capsaicin-like lipid that produces hyperalgesia, J. Biol. Chem. 278 (2003) 13633–13639.
[6] S. Harrison, L. De Petrocellis, M. Trevisani, F. Benvenuti, M. Bifulco, P. Geppetti, V. Di Marzo, Capsaicin-like effects of N-arachidonoyl-dopamine in the isolated guinea pig bronchi and urinary bladder, Eur. J. Pharmacol. 475 (2003) 107–114.
[7] S.E. O'Sullivan, D.A. Kendall, M.D. Randall, Characterisation of the vasorelaxant properties of the novel endocannabinoid N-arachidonoyl-dopamine (NADA), Br. J. Pharmacol. 141 (2004) 803–812.
[8] A. Wojtalla, F. Herweck, M. Granzow, S. Klein, J. Trebicka, S. Huss, R. Lerner, B. Lutz, F.A. Schildberg, P.A. Knolle, T. Sauerbruch, M.V. Singer, A. Zimmer, S.V. Siegmund, The endocannabinoid N-arachidonoyl dopamine (NADA) selectively induces oxidative stress-mediated cell death in hepatic stellate cells but not in hepatocytes, Am. J. Physiol. Gastrointest. Liver Physiol. 302 (2012) G873–G887.
[9] R. Sancho, A. Macho, L. de La Vega, M.A. Calzado, B.L. Fiebich, G. Appendino, E. Munoz, Immunosuppressive activity of endovanilloids: N-arachidonoyl-dopamine inhibits activation of the NF-kappa B, NFAT, and activator protein 1 signaling pathways, J. Immunol. 172 (2004) 2341–2351.
[10] M.Y. Bobrov, A.A. Lizhin, E.L. Andrianova, N.M. Gretskaya, L.E. Frumkina, L.G. Khaspekov, V.V. Bezuglov, Antioxidant and neuroprotective properties of N-arachidonoyldopamine, Neurosci. Lett. 431 (2008) 6–11.
[11] C.M. Navarrete, B.L. Fiebich, A.G. de Vinuesa, S. Hess, A.C. de Oliveira, E. Candelario-Jalil, F.J. Caballero, M.A. Calzado, E. Munoz, Opposite effects of anandamide and N-arachidonoyl dopamine in the regulation of prostaglandin E and 8-iso-PGF formation in primary glial cells, J. Neurochem. 109 (2009) 452–464.
[12] R. Sancho, L. de la Vega, A. Macho, G. Appendino, V. Di Marzo, E. Munoz, Mechanisms of HIV-1 inhibition by the lipid mediator N-arachidonoyldopamine, J. Immunol. 175 (2005) 3990–3999.
[13] C.M. Navarrete, M. Perez, A.G. de Vinuesa, J.A. Collado, B.L. Fiebich, M.A. Calzado, E. Munoz, Endogenous N-acyl-dopamines induce COX-2 expression in brain endothelial cells by stabilizing mRNA through a p38 dependent pathway, Biochem. Pharmacol. 79 (2010) 1805–1814.
[14] S.D. Skaper, V. Di Marzo, Endocannabinoids in nervous system health and disease: the big picture in a nutshell, Philos. Trans. R. Soc. Lond. Ser. B Biol. Sci. 367 (2012) 3193–3200.
[15] R.E. Speer, S.S. Karuppagounder, M. Basso, S.F. Sleiman, A. Kumar, D. Brand, N. Smirnova, I. Gazaryan, S.J. Khim, R.R. Ratan, Hypoxia-inducible factor prolyl hydroxylases as targets for neuroprotection by "antioxidant" metal chelators: from ferroptosis to stroke, Free Radic. Biol. Med. 62 (2013) 26–36.
[16] G.L. Semenza, Life with oxygen, Science 318 (2007) 62–64.
[17] J. Frasor, J.M. Danes, C.C. Funk, B.S. Katzenellenbogen, Estrogen down-regulation of the corepressor N-CoR: mechanism and implications for estrogen derepression of N-CoR-regulated genes, Proc. Natl. Acad. Sci. U. S. A. 102 (2005) 13153–13157.
[18] G.L. Semenza, HIF-1, O(2), and the 3 PHDs: how animal cells signal hypoxia to the nucleus, Cell 107 (2001) 1–3.
[19] P. Jaakkola, D.R. Mole, Y.M. Tian, M.I. Wilson, J. Gielbert, S.J. Gaskell, A. von Kriegsheim, H.F. Hebestreit, M. Mukherji, C.J. Schofield, P.H. Maxwell, C.W. Pugh, P.J. Ratcliffe, Targeting of HIF-alpha to the von Hippel–Lindau ubiquitylation complex by O_2-regulated prolyl hydroxylation, Science 292 (2001) 468–472.
[20] M. Ivan, K. Kondo, H. Yang, W. Kim, J. Valiando, M. Ohh, A. Salic, J.M. Asara, W.S. Lane, W.G. Kaelin Jr., HIFalpha targeted for VHL-mediated destruction by proline hydroxylation: implications for O_2 sensing, Science 292 (2001) 464–468.

Fig. 8. Functional consequences of NADA on the hypoxia response pathway. (A) Human primary astrocytes were stimulated with NADA (10 μM) for 6 h and the expression analysis of genes involved in the human hypoxia signaling pathway determined by PCR array. Heat maps show the significantly upregulated (green) and downregulated (red) genes in NADA-treated cells compared with control. (B) Primary astrocytes were exposed to NADA, hypoxia or both for 6 h and the expression of KH2, BNIP3, HMOX1 and VEGF mRNAs analyzed by qPCR. Data are mean ± SD of n = 3 experiments. $^{*}P < 0.0001$. (C) SK-N-SH cells were stimulated or not with NADA (10 μM) for 3 h, and then subjected or not to hypoxia (1% O_2) for 3 h as indicated. Cell viability was examined by MTT assay. Data are mean ± SD of n = 4 experiments. $^{**}P = 0.0036$. HUVECs (D) or HBMECs (E) were plated on Matrigel-coated culture dishes and treated with NADA (10 μM) for 24 h. Quantitative analysis of tube formation was performed in a BD Pathway 855 Bioimager using Attovission v 1.7 BD software. (D) Data are mean ± SD of n = 3 experiments. $^{**}P = 0.0029$, $^{***}P = 0.0002$ (E) Data are mean ± SD of n = 3 experiments. $^{**}P = 0.0017$.

[21] N. Masson, C. Willam, P.H. Maxwell, C.W. Pugh, P.J. Ratcliffe, Independent function of two destruction domains in hypoxia-inducible factor-alpha chains activated by prolyl hydroxylation, EMBO J. 20 (2001) 5197–5206.
[22] W.C. Hon, M.I. Wilson, K. Harlos, T.D. Claridge, C.J. Schofield, C.W. Pugh, P.H. Maxwell, P.J. Ratcliffe, D.I. Stuart, E.Y. Jones, Structural basis for the recognition of hydroxyproline in HIF-1 alpha by pVHL, Nature 417 (2002) 975–978.
[23] K. Nakayama, I.J. Frew, M. Hagensen, M. Skals, H. Habelhah, A. Bhoumik, T. Kadoya, H. Erdjument-Bromage, P. Tempst, P.B. Frappell, D.D. Bowtell, Z. Ronai, Siah2 regulates stability of prolyl-hydroxylases, controls HIF1alpha abundance, and modulates physiological responses to hypoxia, Cell 117 (2004) 941–952.
[24] A. Moller, C.M. House, C.S. Wong, D.B. Scanlon, M.C. Liu, Z. Ronai, D.D. Bowtell, Inhibition of Siah ubiquitin ligase function, Oncogene 28 (2009) 289–296.
[25] G. Hu, Y.L. Chung, T. Glover, V. Valentine, A.T. Look, E.R. Fearon, Characterization of human homologs of the *Drosophila* seven in absentia (sina) gene, Genomics 46 (1997) 103–111.
[26] K.L. Lorick, J.P. Jensen, S. Fang, A.M. Ong, S. Hatakeyama, A.M. Weissman, RING fingers mediate ubiquitin-conjugating enzyme (E2)-dependent ubiquitination, Proc. Natl. Acad. Sci. U. S. A. 96 (1999) 11364–11369.
[27] J.D. Schnell, L. Hicke, Non-traditional functions of ubiquitin and ubiquitin-binding proteins, J. Biol. Chem. 278 (2003) 35857–35860.
[28] A.H. Tang, T.P. Neufeld, E. Kwan, G.M. Rubin, PHYL acts to down-regulate TTK88, a transcriptional repressor of neuronal cell fates, by a SINA-dependent mechanism, Cell 90 (1997) 459–467.
[29] M.A. Calzado, L. de la Vega, A. Moller, D.D. Bowtell, M.L. Schmitz, An inducible autoregulatory loop between HIPK2 and Siah2 at the apex of the hypoxic response, Nat. Cell Biol. 11 (2009) 85–91.
[30] S. Li, C. Xu, R.W. Carthew, Phyllopod acts as an adaptor protein to link the sina ubiquitin ligase to the substrate protein tramtrack, Mol. Cell. Biol. 22 (2002) 6854–6865.
[31] S.I. Matsuzawa, J.C. Reed, Siah-1, SIP, and Ebi collaborate in a novel pathway for beta-catenin degradation linked to p53 responses, Mol. Cell 7 (2001) 915–926.
[32] T.R. Sarkar, S. Sharan, J. Wang, S.A. Pawar, C.A. Cantwell, P.F. Johnson, D.K. Morrison, J.M. Wang, E. Sterneck, Identification of a Src tyrosine kinase/SIAH2 E3 ubiquitin ligase pathway that regulates C/EBPdelta expression and contributes to transformation of breast tumor cells, Mol. Cell. Biol. 32 (2012) 320–332.
[33] M. Fanelli, A. Fantozzi, P. De Luca, S. Caprodossi, S. Matsuzawa, M.A. Lazar, P.G. Pelicci, S. Minucci, The coiled-coil domain is the structural determinant for mammalian homologues of *Drosophila* Sina-mediated degradation of promyelocytic leukemia protein and other tripartite motif proteins by the proteasome, J. Biol. Chem. 279 (2004) 5374–5379.
[34] H.L. Zhao, N. Ueki, M.J. Hayman, The Ski protein negatively regulates Siah2-mediated HDAC3 degradation, Biochem. Biophys. Res. Commun. 399 (2010) 623–628.
[35] M. Perez, C. Garcia-Limones, I. Zapico, A. Marina, M.L. Schmitz, E. Munoz, M.A. Calzado, Mutual regulation between SIAH2 and DYRK2 controls hypoxic and genotoxic signaling pathways, J. Mol. Cell Biol. 4 (2012) 316–330.
[36] L. Topol, X. Jiang, H. Choi, L. Garrett-Beal, P.J. Carolan, Y. Yang, Wnt-5a inhibits the canonical Wnt pathway by promoting GSK-3-independent beta-catenin degradation, J. Cell Biol. 162 (2003) 899–908.
[37] W. Xie, L. Jin, Y. Mei, M. Wu, E2F1 represses beta-catenin/TCF activity by direct up-regulation of Siah1, J. Cell. Mol. Med. 13 (2009) 1719–1727.
[38] Y. Liao, M. Zhang, B. Lonnerdal, Growth factor TGF-beta induces intestinal epithelial cell (IEC-6) differentiation: miR-146b as a regulatory component in the negative feedback loop, Genes Nutr. 8 (2013) 69–78.
[39] G. Hu, E.R. Fearon, Siah-1 N-terminal RING domain is required for proteolysis function, and C-terminal sequences regulate oligomerization and binding to target proteins, Mol. Cell. Biol. 19 (1999) 724–732.
[40] A. Khurana, K. Nakayama, S. Williams, R.J. Davis, T. Mustelin, Z. Ronai, Regulation of the ring finger E3 ligase Siah2 by p38 MAPK, J. Biol. Chem. 281 (2006) 35316–35326.
[41] J.L. Stebbins, E. Santelli, Y. Feng, S.K. De, A. Purves, K. Motamedchaboki, B. Wu, Z.A. Ronai, R.C. Liddington, M. Pellecchia, Structure-based design of covalent Siah inhibitors, Chem. Biol. 20 (2013) 973–982.
[42] M. Shah, J.L. Stebbins, A. Dewing, J. Qi, M. Pellecchia, Z.A. Ronai, Inhibition of Siah2 ubiquitin ligase by vitamin K3 (menadione) attenuates hypoxia and MAPK signaling and blocks melanoma tumorigenesis, Pigment Cell Melanoma Res. 22 (2009) 799–808.
[43] L. de la Vega, J. Hornung, E. Kremmer, M. Milanovic, M.L. Schmitz, Homeodomain-interacting protein kinase 2-dependent repression of myogenic differentiation is relieved by its caspase-mediated cleavage, Nucleic Acids Res. 41 (2013) 5731–5745.
[44] I.N. Bojesen, H.S. Hansen, Binding of anandamide to bovine serum albumin, J. Lipid Res. 44 (2003) 1790–1794.
[45] K. Nakayama, J. Qi, Z. Ronai, The ubiquitin ligase Siah2 and the hypoxia response, Mol. Cancer Ther. 7 (2009) 443–451.
[46] P. Carmeliet, Y. Dor, J.M. Herbert, D. Fukumura, K. Brusselmans, M. Dewerchin, M. Neeman, F. Bono, R. Abramovitch, P. Maxwell, C.J. Koch, P. Ratcliffe, L. Moons, R.K. Jain, D. Collen, E. Keshert, Role of HIF-1alpha in hypoxia-mediated apoptosis, cell proliferation and tumour angiogenesis, Nature 394 (1998) 485–490.
[47] A. Yamaguchi, M. Taniguchi, O. Hori, S. Ogawa, N. Tojo, N. Matsuoka, S. Miyake, K. Kasai, H. Sugimoto, M. Tamatani, T. Yamashita, M. Tohyama, Peg3/Pw1 is involved in p53-mediated cell death pathway in brain ischemia/hypoxia, J. Biol. Chem. 277 (2002) 623–629.
[48] J. Aragones, P. Fraisl, M. Baes, P. Carmeliet, Oxygen sensors at the crossroad of metabolism, Cell Metab. 9 (2009) 11–22.
[49] O.A. Harari, J.K. Liao, NF-kappaB and innate immunity in ischemic stroke, Ann. N. Y. Acad. Sci. 1207 (2010) 32–40.
[50] M. Winter, D. Sombroek, I. Dauth, J. Moehlenbrink, K. Scheuermann, J. Crone, T.G. Hofmann, Control of HIPK2 stability by ubiquitin ligase Siah-1 and checkpoint kinases ATM and ATR, Nat. Cell Biol. 10 (2008) 812–824.
[51] A. Carlucci, A. Adornetto, A. Scorziello, D. Viggiano, M. Foca, O. Cuomo, L. Annunziato, M. Gottesman, A. Feliciello, Proteolysis of AKAP121 regulates mitochondrial activity during cellular hypoxia and brain ischaemia, EMBO J. 27 (2008) 1073–1084.
[52] E.C. Yego, S. Mohr, siah-1 Protein is necessary for high glucose-induced glyceraldehyde-3-phosphate dehydrogenase nuclear accumulation and cell death in Muller cells, J. Biol. Chem. 285 (2010) 3181–3190.
[53] G. Fiucci, S. Beaucourt, D. Duflaut, A. Lespagnol, P. Stumptner-Cuvelette, A. Geant, G. Buchwalter, M. Tuynder, L. Susini, J.M. Lassalle, C. Wasylyk, B. Wasylyk, M. Oren, R. Amson, A. Telerman, Siah-1b is a direct transcriptional target of p53: identification of the functional p53 responsive element in the siah-1b promoter, Proc. Natl. Acad. Sci. U. S. A. 101 (2004) 3510–3515.
[54] R.J. MacLeod, M. Hayes, I. Pacheco, Wnt5a secretion stimulated by the extracellular calcium-sensing receptor inhibits defective Wnt signaling in colon cancer cells, Am. J. Physiol. Gastrointest. Liver Physiol. 293 (2007) G403–G411.
[55] A. Depaux, F. Regnier-Ricard, A. Germani, N. Varin-Blank, Dimerization of hSiah proteins regulates their stability, Biochem. Biophys. Res. Commun. 348 (2006) 857–863.
[56] M. Scortegagna, T. Subtil, J. Qi, H. Kim, W. Zhao, W. Gu, H. Kluger, Z.A. Ronai, USP13 enzyme regulates Siah2 ligase stability and activity via noncatalytic ubiquitin-binding domains, J. Biol. Chem. 286 (2011) 27333–27341.
[57] I. Grishina, K. Debus, C. Garcia-Limones, C. Schneider, A. Shresta, C. Garcia, M.A. Calzado, M.L. Schmitz, SIAH-mediated ubiquitination and degradation of acetyltransferases regulate the p53 response and protein acetylation, Biochim. Biophys. Acta 1823 (2012) 2287–2296.
[58] S.S.-J. Hu, H.B. Bradshaw, V.M. Benton, J.S.-C. Chen, S.M. Huang, A. Minassi, T. Bisogno, K. Masuda, B. Tan, R. Roskoski Jr., The biosynthesis of *N*-arachidonoyl dopamine (NADA), a putative endocannabinoid and endovanilloid, via conjugation of arachidonic acid with dopamine, Prostaglandins Leukot. Essent. Fat. Acids 81 (2009) 291–301.
[59] K.K. Biswas, K.P. Sarker, K. Abeyama, K.i. Kawahara, S. Iino, Y. Otsubo, K. Saigo, H. Izumi, T. Hashiguchi, M. Yamakuchi, Membrane cholesterol but not putative receptors mediates anandamide-induced hepatocyte apoptosis, Hepatology 38 (2003) 1167–1177.
[60] M. Akimov, I. Nazimov, N. Gretskaya, G. Zinchenko, V. Bezuglov, Sulfation of N-acyl dopamines in rat tissues, Biochem. Mosc. 74 (2009) 681–685.